

1 Supporting Information

2

3

4 **High-resolution Patterned Delivery of Chemical Signals from 3D-printed Picoliter Droplet**

5 **Networks**

6

7 *Jorin Riexinger**, *Thomas Caganek*, *Xingzao Wang*, *Yutong Yin*, *Khoa Chung*, *Linna Zhou*, *Hagan*

8 *Bayley** and *Ravinash Krishna Kumar**

9

10

11

12 **Table of Contents**

13 **Supplementary Notes**

14 Supplementary Note 1: Arabinose-induced Gene Expression: pBAD Rationale

15 Supplementary Note 2: Pattern Fidelity as a Measure of Gene Expression Controllability

16 Supplementary Note 3: Magnetic Beads for Guiding Tissue Placement

17 Supplementary Note 4: *E. coli* Interference Competition

18 Supplementary Note 4.1: Colicin Biology

19 Supplementary Note 4.2: Differences Between Competing Strains

20 Supplementary Note 4.3: Testing Growth Inhibition using Agar Overlay Assay

21 Supplementary Note 4.4: Actively Dividing Cells Are Required for Colicin Competition

22 Supplementary Note 4.5: Droplet Networks and Colicin Competition

23 Supplementary Note 4.6: Importance of Culture Medium for Colicin Competition

24 Supplementary Note 4.7: Local Lysis

25 Supplementary Note 4.8: Colicin E2 Promoter as Indication of DNA Damage

26 **Supplementary Figures**

27 Figure S1: Plasmid maps

28 Figure S2: Magnetic beads guide landing of droplet networks

29 Figure S3: Comparison between droplet networks with and without reservoirs

30 Figure S4: Overlay assay of E7-inducible against colicin E7, colicin E8 and susceptible cells

31 Figure S5: Co-culture of E7-inducible and susceptible cells.

32 Figure S6: Time-dependent release of arabinose from droplet networks

33 Figure S7: Importance of culture medium for colicin competition

34 Figure S8: Localized expression of colicin E7 underneath droplet networks

35 Figure S9: E7-inducible causes DNA damage in susceptible cells

36 Figure S10: Localized DNA damage in susceptible cells by arabinose release from droplet networks

37 **Supplementary Tables**

38 Table S1: Summary of strains and plasmids

39 **Supplementary Methods**

40 Growth Overlay Assay

41 Propidium Iodide Staining

42 Determination of Colony Forming Units (CFU)

43 **References**

45 **Supplementary Notes**

46 **Supplementary Note 1: Arabinose-induced Gene Expression: pBAD Rationale**

47 We chose pBAD as an inducer system for multiple reasons: 1) The permeability of
48 arabinose (chemical signal) was minimal (Figure 1(h)) through lipid bilayers (comprising of a
49 lipid composition 2:1 (molar ratio) DPhPC:POPC) formed between compartments within
50 droplet networks (droplet interface bilayers = DIBs) and between droplet networks and the
51 hydrogel (droplet hydrogel bilayers = DHBs). This allowed us to control the arabinose flux
52 from the droplet networks into the bacterium-laden hydrogels by changes in both arabinose
53 and α HL concentration, and prevented diffusion of arabinose between compartments within
54 the droplet networks unless α HL was present in the DIBs. 2) pBAD systems have been
55 reported to behave as an all-or-nothing system,^[1] which we reasoned would be ideal to
56 achieve patterned gene expression based on arabinose flux from droplet networks. We
57 hypothesized that below or above a critical arabinose concentration, the gene expression in
58 cells would be low and high, respectively, rather than a gradient going from low to high.
59 Hence, a tight population gene expression pattern could be achieved depending on the
60 arabinose gradient released over time. This all-or-nothing system works once a critical
61 concentration of arabinose is reached, resulting in high expression levels of genes
62 downstream of the P_{BAD} promoter, such as *mCherry* or *cxE7*. At the same time, increased
63 activity of the transcriptional regulator AraC induces the expression of *araE*, which encodes
64 for the arabinose transporter AraE. This increases the uptake of arabinose, leading to a
65 positive feedback loop that rapidly increases protein expression in the cells until a maximum
66 is reached.

67

68 **Supplementary Note 2: Pattern Fidelity as a Measure of Gene Expression** 69 **Controllability**

70 As described, our *PF* measure describes the controllability of gene expression in *E. coli*
71 populations by comparing the area of unintended gene expression, A_U , to the area of intended
72 gene expression, A_I . Another measure we considered was factoring A_N , which refers to the
73 area within A_I , where no gene expression was induced. However, this measure was not
74 chosen to optimize arabinose release from 3D-printed droplet networks, as we did not
75 encounter areas within A_I where gene expression was not induced (unless droplets did not
76 form DHBs with the hydrogel (see Figure 3(g))). Therefore, our *PF* measure was chosen to
77 quantify gene expression in areas outside of the intended gene expression area as a measure

78 over controlled release of arabinose. However, in addition we reported values of
79 A_N (Figure 2(g)), which takes into account areas within A_I where insufficient DHB formation
80 as a consequence of printing defects and irregularities of the surface of bacterium-laden
81 hydrogels prevented arabinose release.

82

83 By using cascade blue dextran to reveal where arabinose was released from droplet networks,
84 we could determine the area of unintended gene expression, A_U and A_N (Figure 2(a)).
85 However, in some cases, the definitive location of arabinose release was imperfect due to
86 imaging limitations.^[2] This is because the layers of droplets in our droplet networks are
87 stacked by shifting every other layer in both the x - and y -directions such that hexagonally-
88 packed structures can form. So, droplets of the same position in x and y within the droplet
89 networks were offset depending on the layer. Therefore, accurate determination of the
90 droplets from which arabinose was being released into the bacterium-laden hydrogel was
91 difficult in some cases. In particular, this may cause inaccuracies in locating fine patterns,
92 such as single-droplet diffusive pathways (Figure 4(b)) or patterns in mask layers, where the
93 fluorescence signal from cascade blue dextran in droplets comprising reservoir layers may
94 interfere with the fluorescence signal from cascade blue dextran droplets in the mask
95 layers (Figure S4 and S5).

96

97 **Supplementary Note 3: Magnetic Beads for Guiding Tissue Placement**

98 Our 3D droplet printing technology can be time-consuming when printing intricate patterns.
99 This is because, 1) droplets are positioned one after another, 2) when printing droplets of
100 different compositions (e.g. with or without arabinose and α HL), two printing nozzles are
101 used of which the printing stage has to be moved between the nozzle positions. For example,
102 printing droplet networks composed of $10 \times 10 \times 8$ droplets (in xyz -direction) takes 67
103 minutes for a cross-like pattern and 87 minutes for an arrow-like pattern. To overcome this,
104 we reasoned that only the bottom layers (masks) in the droplet networks are necessary to be
105 patterned, as long as this ‘mask’ layer was connected to a reservoir of arabinose and α HL-
106 containing droplets to supply arabinose to the mask layers. Therefore, we printed cubic,
107 arabinose-containing ‘reservoirs’ (4-8 layers) on top of the mask layers (4 layers) connecting
108 reservoirs to the mask via α HL-mediated droplet diffusive pathways. Using this method, we
109 reduced our printing time significantly, for example, the printing time for droplet networks
110 composed of twelve cross-like patterned layers ($9 \times 9 \times 12$ droplets) was 56 minutes, while

111 the printing time for droplet networks composed of 4 mask layers ($9 \times 9 \times 4$ droplets) of the
112 same pattern and 8 reservoir layers ($7 \times 7 \times 8$) on top was 41 minutes. Moreover, this method
113 stored arabinose more efficiently within the droplet network in terms of occupied volume, as
114 8 reservoir layers were composed of a total of 392 α HL and cascade blue dextran-containing
115 droplets as opposed to 136 in 8 patterned layers.

116

117 To avoid reservoir droplets from accidentally rolling to the patterned bottom layer of droplet
118 networks during printing and, hence, disrupting intended patterns, reservoirs were designed to
119 be slightly smaller than bottom layers (e.g. 6×6 droplets (reservoir) instead of 8×8
120 droplets (mask)). As a result, we found that droplet networks predominantly flipped before
121 they landed on top of the bacterium-laden hydrogel (i.e. the reservoir interfaced with the
122 hydrogel instead of the mask layer, Figure S2(a)). Out of 45 droplet networks composed of
123 patterned masks and a reservoir, 88.9% flipped during the transfer and landed with the
124 reservoir facing the hydrogel. In this case, arabinose would diffuse directly from the reservoir
125 to the cells, resulting in gene expression patterns reflecting the shape of the reservoir, rather
126 than the intended pattern (Figure S2(b)). This occurred likely due to hydrodynamic forces in
127 the viscous lipid-in-oil solution, aligning the smaller reservoir towards the hydrogel. To
128 overcome the flipping, we developed a mechanism to control the landing of droplet networks
129 on top of the hydrogel. This comprised of attaching droplets containing magnetic
130 beads (1.5% w/v ultra-low gelling agarose and nickel magnetic beads) to the corners of the
131 mask layers before the transfer and then placing a magnet underneath the bacterium-laden
132 hydrogel to guide the mask layer towards the hydrogel. Using this method, the correct
133 landing was achieved in 76.5% of 34 transferred droplet networks, allowing for patterned
134 gene expression in bacterial cells by the mask layers rather than the reservoir
135 layers (Figure S2(c)).

136

137 Next, we investigated the number of mask layers that were necessary to consistently induce
138 patterned gene expression. We printed droplet networks composed of 1, 2, 3 and 4-layered
139 masks comprising a stripe-like pattern and an 8-layered reservoir on top (33 mM arabinose
140 and $50 \mu\text{g mL}^{-1}$ α HL). Accordingly, 4 connected mask layers were necessary to induce stripe-
141 like gene expression in bacterial cells (Figure 3(d)-Figure 3(g) and Figure S2(d)).

142

143 Finally, we compared gene expression patterns induced by arabinose release from droplet
144 networks with and without reservoirs. Droplet networks with reservoirs consisted of 4-

145 layered masks encoding for a single-droplet pathway and 4-layered reservoirs on
146 top (Figure S3(a)), whereas droplet networks without reservoirs consisted of 8-layered masks
147 encoding for a single-droplet pathway. Using both types of droplet networks (with and
148 without reservoirs), single-droplet gene expression patterns could be induced. Further, we
149 found that there was no significant difference between droplet network type regarding *PF* and
150 mean mCherry expression (Figure S3(b)), confirming that droplet networks composed of
151 masks and reservoirs are not only more efficient in terms of printing time and occupied space
152 but also induced gene expression at similar spatial resolution compared to droplet networks
153 comprised completely of mask layers.

154

155 **Supplementary Note 4: *E. coli* Interference Competition**

156 Supplementary Note 4.1: Colicin biology

157 *E. coli* can produce colicins, protein toxins that target susceptible *E. coli* strains, which is
158 crucial for interference competition between strains.^[3,4] These colicins, specifically group A
159 colicins (E7, E8), are encoded on a plasmid (pCol, type I plasmids: 6–10 kb) with about 20
160 copies per cell. Type I plasmids carry group A colicins, which parasitize the Ton system in *E.*
161 *coli* for entry into the periplasm. Group A colicins include nuclease colicins (E7, E8) causing
162 DNA damage to susceptible cells which mostly cause cell death.^[5]

163

164 On the pCol plasmid, the colicin operon is controlled by the LexA protein, which represses
165 the SOS promoter. The SOS response, triggered by DNA damage, upregulates RecA,
166 enabling LexA self-cleavage. This allows RNA polymerase binding to the SOS promoter for
167 colicin operon transcription, leading to colicin expression. Nuclease colicins are associated
168 with two genes: one encoding the colicin and the other the cognate immunity protein. The
169 immunity protein is constitutively expressed, preventing self-intoxication. Last, the operon
170 also contains a gene that encodes the lysis protein needed for colicin release.^[5]

171

172 Supplementary Note 4.2: Differences Between Competing Strains

173 We utilized six distinct strains in our inducible competition assays:

174 1) S (BZB1011): a susceptible strain to DNA damage (and as a consequence, likely
175 death) by colicins E7 and E8. It does not carry a colicin-producing plasmid (Table S1,

176 2)

- 177 2) S-GFP (BZB1011 pUA66-PcolE2::gfp): a susceptible strain to DNA damage (and as
178 consequence, likely death) by colicins E7 and E8. It also does not carry a colicin-
179 producing plasmid but, but harbours a DNA damage-reporting plasmid (Table S1, 5)
180 3) E7-inducible (BZB1011 pKC1-PBAD:-ColE7-AMP): a strain that upregulates the
181 colicin E7 operon (toxin, immunity, and lysis proteins) in the presence of arabinose,
182 and is susceptible to colicin E8 (Table S1, 3)
183 4) E7R-inducible (BZB1011 pYY1-PBAD:-ColE7-mCherry-AMP): a strain that
184 upregulates the colicin E7 operon (toxin, immunity, and lysis proteins) and the
185 mCherry protein in the presence of arabinose, and is susceptible to colicin E8 (Table
186 S1, 4)
187 5) E7 (BZB1011 pColE7): the natural colicin E7-producing strain that upregulates the
188 colicin E7 operon when experiencing DNA damage, and is susceptible to colicin
189 E8 (Table S1 , 6)
190 6) E8 (BZB1011 pColE8): the natural colicin E8-producing strain that upregulates the
191 colicin E8 operon when experiencing DNA damage, and is susceptible to colicin
192 E7 (Table S1, 7).

193 Notably, colicin-producing strains (E7-inducible, E7R-inducible, E7 and E8) possess
194 additional mechanisms for toxin release. These strains exhibit a basal toxin production rate.
195 For E8, approximately 1 in 200 cells stochastically upregulate toxin and lysis protein
196 production^[5]; the basal rate is assumed to be lower for the E7-inducible strain. Specifically
197 for the natural colicin E8 producer, E8 can amplify toxin production through autoinduction.
198 This density-dependent mechanism involves clonemates being more likely to upregulate their
199 colicin E8 operon when in the proximity of an E8 cell that releases toxins. This occurs
200 because E8 produces lower amounts of cognate immunity protein so that the probability of
201 DNA damage is increased upon import of a clonemates' released colicin E8.^[5]

202

203 Supplementary Note 4.3: Testing Growth Inhibition Using Agar Overlay Assay

204 To test whether our E7-inducible (BZB1011 pKC1-PBAD:-ColE7-AMP) strain expressed
205 colicin E7 upon induction with arabinose, we performed overlay assays (Figure S4(a)-(d), see
206 Supplementary Methods), where E7-inducible cells were spotted on top of cells that natively
207 produce colicin E7 (BZB1011 pColE7 – E7), (Table S1, 6) or colicin E8 (BZB1011 pColE8 –
208 E8), (Table S1, 7) and susceptible cells (BZB1011 – S), (Table S1, 2). Using an agar overlay
209 assay^[6] when E7-inducible was spotted on top of an E7 top agar, E7-inducible continued to

210 grow when no arabinose was added to the plates. Adding arabinose concentrations of
211 0.5% (w/v), 1% (w/v) and 5% (w/v) to the agar caused complete lysis of E7-inducible. In
212 contrast, E7 continued to grow at all arabinose concentrations used (0% (w/v) to 5% (w/v)),
213 due to it expressing the E7 immunity protein (Figure S4(a)).

214

215 When E7-inducible was spotted on E8 top agar, no growth was observed of E7-inducible
216 after 18 h (Figure S4(b)). We reasoned this was because of the higher basal expression of E8
217 compared to E7-inducible, and E8's ability to respond to an attack from E7 as the natural
218 operon is upregulated by DNA damage. Taken together E8 is dominant because it can
219 produce a lot more toxin than the uninduced E7-inducible strain (see colicin biology section).

220

221 With arabinose concentrations of $\geq 0.5\%$ (w/v) in the agar, E7-inducible was activated,
222 leading to not only mass lysis of E7-inducible (as the entire colicin operon, including the lysis
223 protein is under control of the P_{BAD} promoter), but also growth inhibition in native colicin E8-
224 expressing cells, because of the high concentration of colicin E7 released from E7-inducible
225 cells (Figure S4(b)).

226

227 In the case where E7-inducible was spotted on top of LB agar containing susceptible
228 cells (BZB1011 – S), E7-inducible continued to grow when no arabinose was present.
229 However, a halo around the location where E7-inducible was spotted, presumably because of
230 low basal levels of E7 expression in LB medium, affecting susceptible cells at the boundary
231 of the E7-inducible spot (Figure S4(c)). In contrast, when E7-inducible was spotted on top of
232 M9 agar containing susceptible cells (BZB1011 – S), both E7-inducible and S cells grew next
233 to each other when no arabinose was present (Figure S4(d)). As soon as arabinose was added
234 to the plates ($\geq 0.5\%$ (w/v)) E7-inducible was activated, leading to growth inhibition of
235 susceptible cells both in LB agar plates (Figure S4(c)) and in M9 medium agar
236 plates (Figure S4(d)).

237

238 Supplementary Note 4.4: Actively-Dividing Cells Are Required for Colicin Competition

239 Next, we investigated whether growth of susceptible cells can be inhibited by induced
240 expression of colicin E7 at a range of arabinose concentrations (0 mM to 333 mM) when both
241 cells were mixed homogeneously at an equal starting ratio (1:1) in M9 ultra-low gelling
242 agarose (ULGA, 1.5% w/v). At a total starting cell density of 3.6×10^9 cells mL⁻¹ the mean

243 GFP expression of E7-inducible, arising from constitutive expression of GFP, decreased only
244 slightly with increasing arabinose concentrations (Figure S5(a)), indicating a low number of
245 lysis events and, hence, minimal expression of colicin E7. This is supported by the fact that
246 the mean RFP expression of susceptible cells, arising from constitutive expression of RFP,
247 did not decrease significantly with increasing arabinose concentrations (Figure S5(a)). We
248 hypothesized that colicin E7 expression was low because not many cell divisions of the E7-
249 inducible strain occurred in the hydrogel at these high cell densities.

250

251 To confirm whether lower cell densities, and hence whether sustained cell divisions during
252 interference competition is required for E7-inducible to express colicin E7 in M9 ULGA, we
253 decreased the starting cell density of E7-inducible to 1.6×10^7 cells mL⁻¹ within the hydrogel.
254 Indeed, the number of micro-colonies arising from E7-inducible decreases with increasing
255 arabinose concentrations within the M9 ULGA gels, suggesting induced expression of colicin
256 E7 lysis protein at lower cell densities (Figure S5(b)). Similarly, when both E7-inducible and
257 susceptible cells were mixed homogeneously at equal starting ratio and a combined starting
258 cell density of 1.6×10^7 cells mL⁻¹ the number of E7-inducible micro-colonies decreased with
259 increasing arabinose concentrations. No micro-colonies were observed of susceptible cells
260 after 18 hours of co-culture, which suggests that baseline expression levels of colicin E7 in
261 the absence of arabinose was sufficient to inhibit the growth of susceptible
262 cells (Figure S5(c)). Hence, the homogeneous distribution of E7-inducible and susceptible
263 cells in our bacterium-laden hydrogel enhanced the effect of colicin E7 baseline expression
264 compared to the agar overlaying assay.

265

266 Therefore, we decreased the starting ratio from initially 1:1 to 1:9 and 1:99 (number of E7-
267 inducible cells to number of susceptible cells). At a starting ratio of 1:9 and total starting cell
268 density of 1.6×10^7 cells mL⁻¹ both E7-inducible and susceptible cells grew to
269 homogeneously-distributed micro-colonies within M9 ULGA gels when no arabinose was
270 present (Figure S5(d)). With increasing arabinose concentrations both the number of E7-
271 inducible and susceptible micro-colonies decreased, suggesting both lysis of E7-inducible
272 and DNA-damaging effects on S cells. At a starting ratio of 1:99 of E7-inducible to
273 susceptible cells, less susceptible cells were inhibited presumably because of the much lower
274 starting densities of E7-inducible and hence lower release concentrations colicin
275 E7 (Figure S5(e)).

276

277 Supplementary Note 4.5: Droplet Networks and Colicin Competition

278 From our above results, we hypothesized that arabinose released from droplet networks into
279 bacterium-laden M9 ULGA gels (supplemented with 24 mM glucose) could induce localized
280 lysis of E7-inducible cells that would, in turn, clear a localized area of susceptible cells when
281 the two strains were incubated at a starting ratio of 1:9. Therefore, we placed droplet
282 networks containing 33 mM arabinose and 50 $\mu\text{g mL}^{-1}$ αHL on top of bacterium-laden
283 hydrogels containing E7-inducible and S cells. Droplet networks were placed either
284 immediately after the gels were formed or 24 h after the gels were formed. However, when
285 droplet networks were placed after the gels were formed, the number of micro-colonies of both
286 E7-inducible and susceptible cells did not change significantly, indicating that arabinose
287 release from droplet networks did not induce levels of colicin E7 required for clearing of
288 susceptible cells. The time point of tissue placement in regards to formation of the gel (just
289 after or 24 hours after formation) did not affect the final number of E7-inducible and S
290 cells (Figure S6(a) and (b)).

291

292 We reasoned higher concentrations of arabinose within droplet networks were required to
293 induce sufficient expression of colicin E7 in E7-inducible. However, a ten-fold increase in
294 arabinose concentration (333 mM) did not lead to lysis of E7-inducible within 42 h of the
295 competition assay against S cells, as confirmed by the number of micro-colonies arising from
296 E7-inducible cells (Figure S6(c)). Therefore, the number of micro-colonies arising from
297 susceptible cells did not change significantly when comparing droplet networks with or
298 without arabinose (Figure S6(d)).

299

300 Supplementary Note 4.6: Importance of Culture Medium for Colicin Competition

301 We wondered whether the culture medium in the gels had a significant impact on induced
302 gene expression of E7-inducible. In particular, we hypothesized that glucose, which was
303 supplemented to M9 as a carbon source throughout previous experiments, could act as
304 catabolic repressor, limiting gene expression levels.^[7,8] Our hypothesis was based on the
305 differences in basal expression of E7-inducible from overlay assays (Figure S4(c) and S4(d)),
306 where without addition of arabinose E7-inducible visibly inhibited and did not visibly inhibit
307 S cells when LB and M9 medium were used, respectively. To test these effects of media
308 composition on colicin expression in E7-inducible, we monitored cell lysis in E7-inducible
309 populations in ULGA gels (at a starting cell density of 3.6×10^9 cells mL^{-1}) composed of M9

310 supplemented with 24 mM glucose, M9 supplemented with 24 mM glycerol or LB at
311 arabinose concentrations of 0 mM, 6 mM, 33 mM and 66 mM. We monitored cell lysis by
312 tracking constitutive sfGFP expression (on the chromosome of E7-inducible), as and
313 indication of cell viability, and propidium iodide staining in E7-inducible, as indication of
314 cell death, which has previously been shown to confirm cell lysis.^[3] A decrease in sfGFP
315 expression and increase in propidium iodide fluorescence would indicate cell lysis (as
316 propidium iodide can only penetrate cells and bind to DNA when the membrane is
317 compromised). While the mean gene expression of sfGFP did not change significantly when
318 comparing glucose and glycerol as supplemented carbon source in M9 medium, a significant
319 decrease in sfGFP was observed for gels composed of LB with increasing arabinose
320 concentrations (Figure S7(a)). Moreover, propidium iodide fluorescence increased when cells
321 were in LB medium supplemented with arabinose as compared to M9 medium, indicating
322 increased cell lysis (Figure S7(b)). The combination of decreased sfGFP expression and
323 increased propidium iodide intensity indicated a significant reduction in number of micro-
324 colonies formed with increasing arabinose concentrations. Interestingly, the propidium ioide
325 fluorescence was significantly increased for gels composed of M9 supplemented with
326 glycerol at arabinose concentrations of 33 mM and 66 mM compared to gels supplemented
327 with glucose, indicating increased cell lysis in the presence of glycerol as compared to
328 glucose (Figure S7(b)).

329

330 Supplementary Note 4.7: Local Lysis

331 Next, we investigated whether E7-inducible cells could be lysed when droplet networks
332 containing 333 mM of arabinose and 50 $\mu\text{g mL}^{-1}$ of αHL monomer were placed on top of
333 bacterium-laden hydrogels composed of LB ULGA. For this we formed gels containing E7-
334 inducible at a starting cell density of 1.6×10^7 cells mL^{-1} and measured the number of micro-
335 colonies in the periphery and center when droplet networks were or were not placed on top of
336 the bacterium-laden hydrogels (Figure S8(a) and Figure S8(b)). Center refers to the area
337 directly underneath droplet networks and the same areas when no droplet networks were
338 placed, whereas periphery refers to the area outside of where droplet networks were
339 placed (Figure S8(a)). So, droplet networks were used as reference region of interest both
340 when droplet networks were placed on top of the bacterium-laden hydrogel (+ST) or when
341 droplet networks were not placed on top(-ST). Critically, the cell density of E7-inducible
342 cells was significantly reduced both in the periphery and center when droplet networks were

343 placed on top of the bacterium-laden hydrogel compared to when no droplet networks were
344 present (Figure S8(b)), suggesting that local lysis of E7-inducible is indeed possible when
345 arabinose is released from droplet networks in LB.

346

347 As the localized expression of colicin E7 was achieved in LB, we investigated the effect of
348 toxin release on susceptible cells at different starting ratios. Here, the total starting cell
349 density was kept constant at 1.6×10^7 cells mL⁻¹, while altering the starting ratio of E7-
350 inducible to susceptible cells from 1:9 to 9:1. We found that the relative abundance of E7-
351 inducible decreased when droplet networks containing 333 mM of arabinose and 50 µg mL⁻¹
352 of αHL monomer were placed on top of the bacterium-laden hydrogel (Figure S8(c)).
353 However, the cell density of susceptible cells was not affected significantly when droplet
354 networks were placed on top of the bacterium-laden hydrogel as compared to when they were
355 not. Taken together, these results indicated that the initial assumption of distinctive cell
356 clearing of susceptible cells as a consequence of induced E7 expression may be limited
357 within the time course of our experiments.

358

359 Supplementary Note 4.8: Colicin E2 Promoter as Indication of DNA Damage

360 From our experiments, we thought a susceptible strain was needed to report on DNA damage
361 as an indication of cell inhibition, rather than focusing on cell clearing. We reasoned that the
362 natural promoter of colicin-expressing strains, which is regulated by DNA damage (see
363 colicin biology section), could act as reporter of DNA damage in susceptible cells. Therefore,
364 we transformed susceptible cells with a reporter plasmid (pUA66-*P_{colE2}:sfGFP*)^[3,4] which
365 allowed us to monitor the activity of *P_{colE2}* based on GFP expression levels and, hence, levels
366 of DNA-damage that susceptible cells may experience as a consequence of induced colicin
367 E7 expression. In summary, susceptible cells (S-GFP) would express GFP in response to
368 DNA-damage. Additionally, to track colicin operon activity in the E7-inducible strain, we
369 created a reporter strain with *mCherry* downstream of the colicin E7 lysis gene, i.e. when the
370 operon was active, fluorescent protein would be produced (BZB1011 *pYY1-PBAD:-ColE7-*
371 *mCherry-AMP*, E7R-inducible).

372

373 First, we mixed E7R-inducible cells and S-GFP cells at equal starting ratio and a total starting
374 cell density of 1.6×10^7 cells mL⁻¹, or S-GFP cells only at a starting cell density of
375 0.8×10^7 cells mL⁻¹, in M9 ULGA gels supplemented with 24 mM of glycerol and a range of

376 arabinose concentrations (0 mM to 8 mM, Figure S9(a)). After 18 hours of culture at 37°C we
377 found that mCherry expression increased with increasing arabinose concentrations, indicating
378 increasing levels of colicin E7 expression with increasing concentrations of
379 arabinose (Figure S9(b)). The mean GFP expression in S-GFP cells increased significantly at
380 arabinose concentrations of 0.25 mM and 0.5 mM in the gels as compared to when no
381 arabinose was present in the gels. However, a further increase of arabinose (>0.5 mM)
382 concentration caused a significant drop in GFP expression (Figure S9(b)), of which we
383 assumed cells were killed too quickly (with high concentrations of expressed colicin E7) to
384 report on DNA-damage. To correlate GFP expression with the ability of S-GFP cells to
385 replicate, we re-suspended cells from the ULGA gels and plated them on selective LB agar
386 plates (with kanamycin selecting for S-GFP cells) and measured the relative number of
387 colony forming units (R_{CFU}) of S-GFP cells after 12 hours at 37°C:

$$388 \quad R_{CFU} = \frac{N_{CFU}}{N_{CFU_{single}}} 100\%, \quad (S1)$$

389 where N_{CFU} refers to the number of colony forming units at a certain concentration of
390 arabinose in the gels before plating (0 mM to 8 mM) and $N_{CFU_{single}}$ refers to the number of
391 colony forming units when only S-GFP cells were seeded in ULGA gels without E7R-
392 inducible cells and without arabinose (single). We found a significant drop in R_{CFU} at an
393 arabinose concentration of 0.5 mM in the ULGA gels, confirming that the observed increase
394 in GFP indeed was an indication of cell inhibition of S-GFP cells.

395

396 From this, we printed droplet networks containing $50 \mu\text{g mL}^{-1}$ of αHL monomer and a range
397 of arabinose concentrations (0 mM to 33 mM) and placed them on top of homogeneously-
398 distributed cells of E7R-inducible and S-GFP cells at equal starting ratio and a total cell
399 density of $1.6 \times 10^7 \text{ cells mL}^{-1}$. We did not observe any DNA damage in S-GFP cells when
400 droplet networks contained ≤ 3 mM of arabinose. However, at 16 mM of arabinose the number
401 of micro-colonies of S-GFP cells that experienced DNA damage increased significantly, both
402 underneath the droplet network and in the periphery. Further increase in arabinose (33 mM)
403 led to a decrease in the number of micro-colonies expressing sfGFP, suggesting decreased
404 viability, i.e. cells were inhibited too quickly to report on DNA-damage (Figure S9(c)).

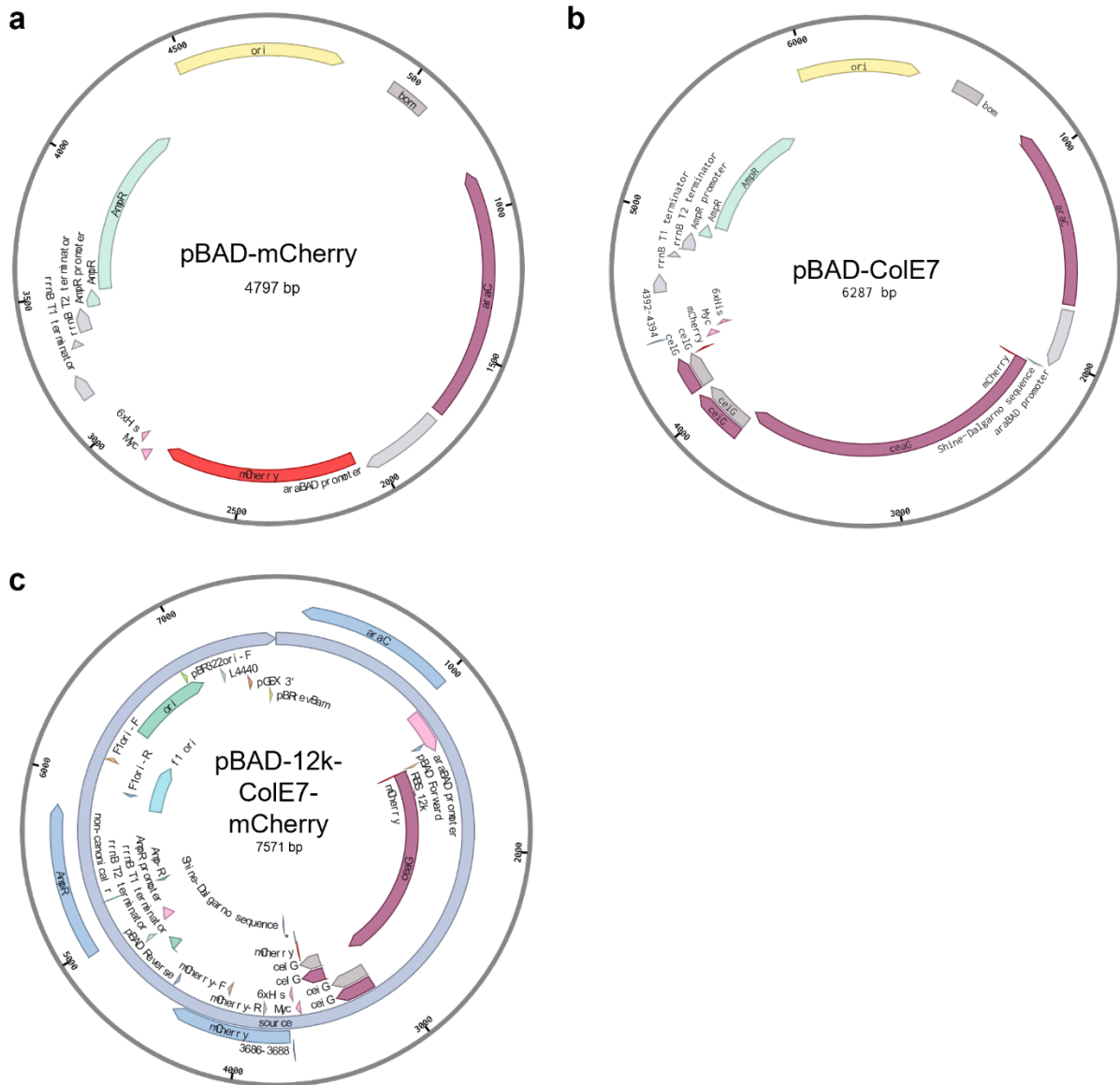
405

406 In order to achieve patterned DNA damage in S-GFP cells, we adjusted both
407 arabinose (8 mM, 12 mM and 16 mM) and αHL monomer concentrations ($0 \mu\text{g mL}^{-1}$,

408 10 $\mu\text{g mL}^{-1}$, 25 $\mu\text{g mL}^{-1}$ and 50 $\mu\text{g mL}^{-1}$) so to control the release of arabinose from droplet
409 networks. With increasing arabinose and αHL concentrations the number of S-GFP cells
410 experiencing DNA-damage increased both underneath droplet networks (Figure S10(a)), and
411 outside of where droplet networks were placed (Figure S10(b)). Moreover, the mean sfGFP
412 expression increased with increasing arabinose and αHL concentrations (Figure S10(c)),
413 while the mean micro-colony 2D cross-sectional area of S-GFP cells increased up to
414 198.5 μm^2 before it decreased to 63.7 μm^2 (Figure S10(d)).

415

416 **Supplementary Figures**
 417



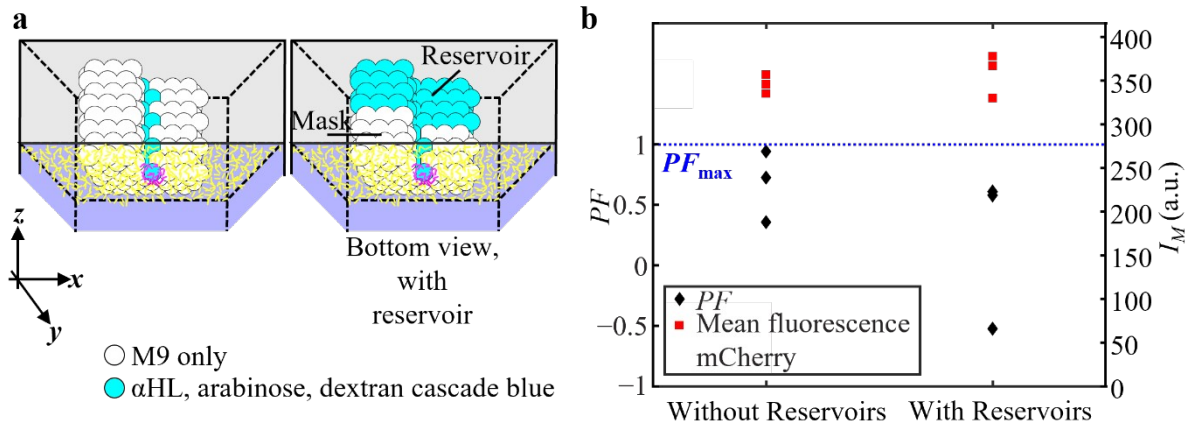
418
 419 **Figure S1.** Plasmid maps of plasmids used throughout this work. (a)-(c) Schematics of
 420 plasmid maps of pJS1-PBAD:-mCherry-AMP, pKC1-PBAD:-ColE7-AMP and pYY1-
 421 PBAD:-ColE7-mCherry-AMP, respectively. Plasmid maps were created using Benchling.^[9]

422

430 we reasoned drives the flipping process as the reservoir is smaller in size compared to the
431 mask. (b) Schematic of a droplet network that flips and lands reservoir side down activating
432 expression of mCherry in the bacterial population. Bottom right microscopy images (bright-
433 field and epi-fluorescence) is an example of a droplet network landing reservoir side down
434 onto the bacterium-laden hydrogel. Images were taken 18 hours after placement of the droplet
435 network (containing 33 mM arabinose and $50 \mu\text{g mL}^{-1}$ αHL monomer). Cyan fluorescence
436 represents cascade blue dextran, while magenta fluorescence represents mCherry expression.
437 (c) Schematic of a droplet network that does not flip and lands mask side down due to
438 magnetic beads (droplets composed of 1.5% w/v ultra-low gelling agarose and nickel
439 magnetic beads) attached to each corner of the mask of a droplet network and a magnet
440 placed underneath the bacterium-laden hydrogel during tissue transfer. The release of
441 arabinose from the mask of a droplet network containing 33 mM arabinose and $50 \mu\text{g mL}^{-1}$
442 αHL monomer activated patterned (cross-like shape) expression of mCherry in the bacterial
443 population. Bottom right microscopy images (bright-field and epi-fluorescence) is an
444 example of a droplet network landing mask side down onto the bacterium-laden hydrogel.
445 Images were taken 18 hours after droplet network placement and cyan and magenta
446 fluorescence represent cascade blue dextran and mCherry expression, respectively. (a)-(c) In
447 droplet networks cyan droplets contained 33 mM arabinose, $50 \mu\text{g mL}^{-1}$ αHL monomer, and
448 $250 \mu\text{M}$ cascade blue dextran, whereas grey droplets did not contain these components.
449 (d) Epi-fluorescent microscopy images depicting mCherry expression (magenta) induced by
450 the release of arabinose from droplet networks composed of 1, 2, 3 or 4 mask layers (stripe-
451 like pattern) and 4 reservoir layers 18 hours after tissue placement on top of the bacterium-
452 laden hydrogel. The droplets within the stripe-like pattern of the mask and all reservoir
453 droplets contained 33 mM arabinose, $50 \mu\text{g mL}^{-1}$ αHL monomer, and $250 \mu\text{M}$ cascade blue
454 dextran, whereas droplets of mask layers located outside the stripe-like pattern did not
455 contain these components. Shown are $n = 4$ replicates.

456

457

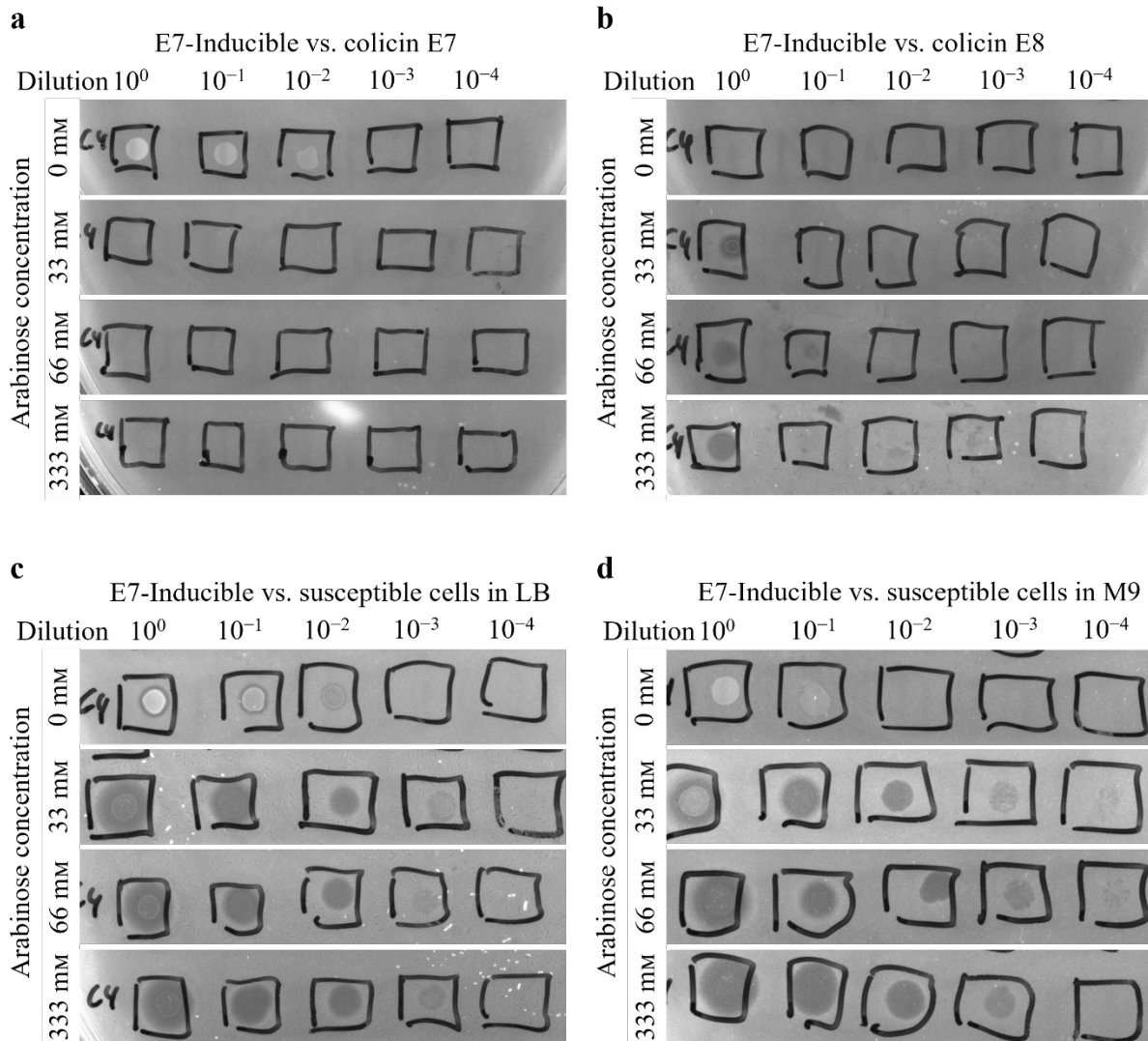


458

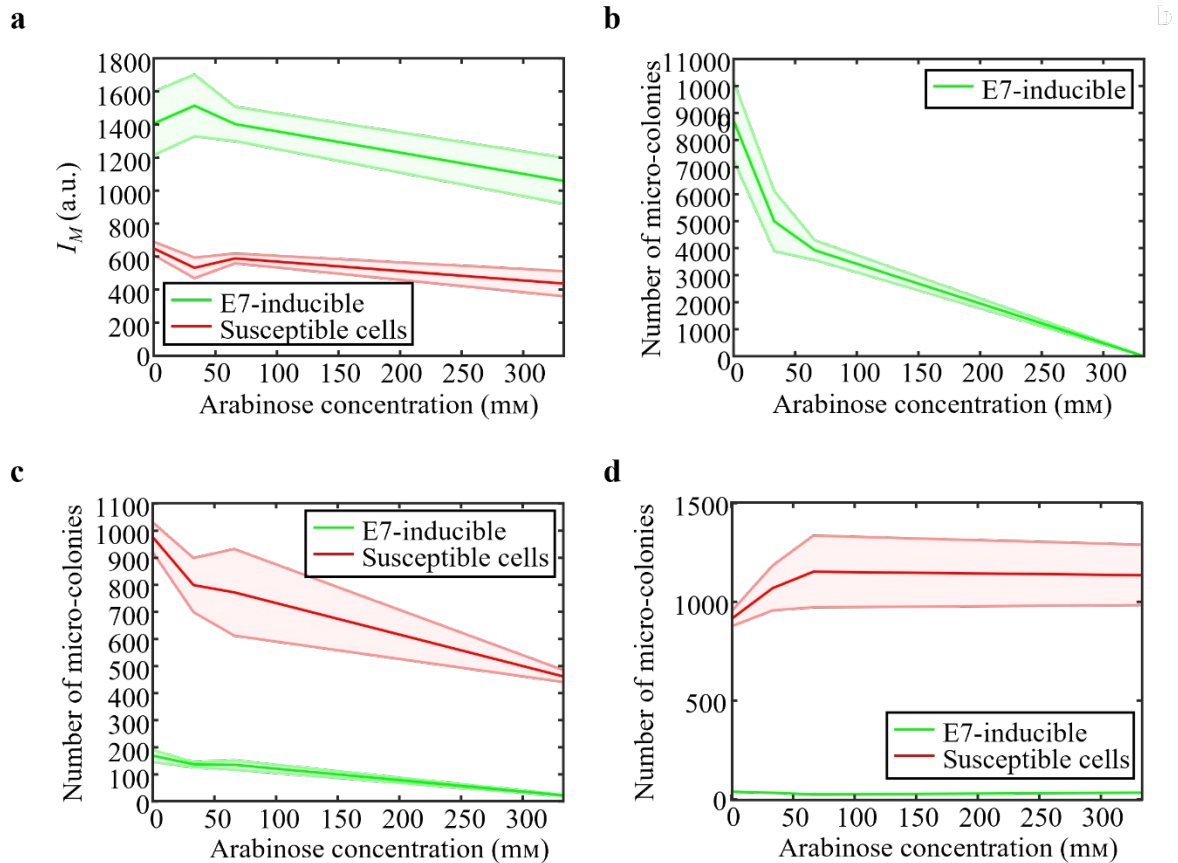
459

Figure S3. Single-droplet gene expression with and without reservoirs. (a) Schematic illustrating droplet networks composed of 8 patterned layers (without reservoirs) or 4 patterned mask layers and 4 reservoir layers (with reservoirs). Both types of droplet networks were composed of droplets that contained 33 mM arabinose and $50 \mu\text{g mL}^{-1}$ α HL monomer (cyan droplets) or did not contain these components (white droplets). (b) Graph of the PF and mean mCherry expression induced by arabinose release from droplet networks with and without reservoirs on top of masks comprising of a single-droplet diffusive pathway that contacts the hydrogel surface forming a DHB.

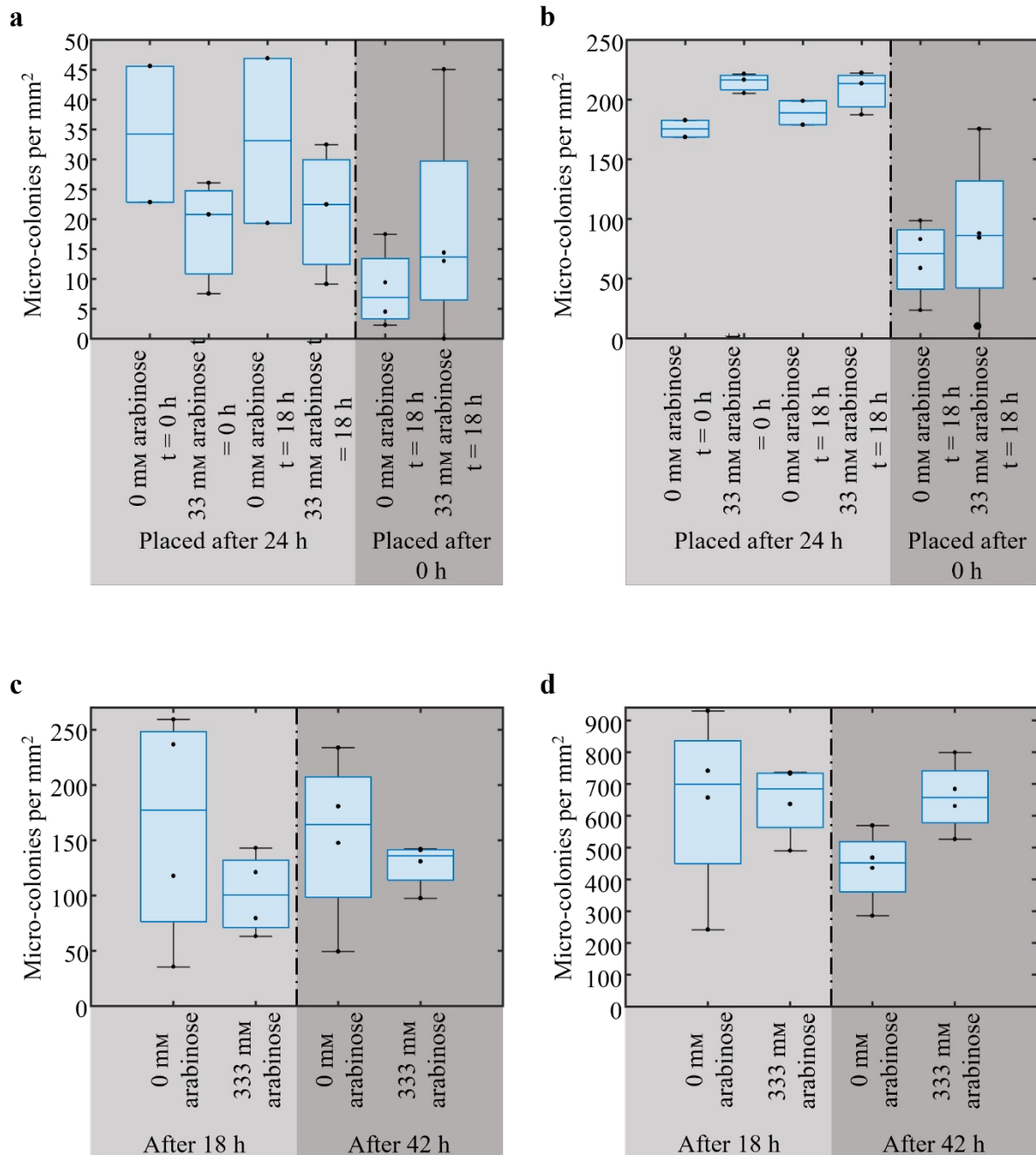
467



470
471 **Figure S4.** Overlay assay of E7-inducible against colicin E7, colicin E8-expressing and
472 susceptible cells. (a) – (d) Photographs of serial dilutions from 10^0 to 10^{-4} (of an overnight
473 liquid culture) of E7-inducible (BZB1011 pBAD-E7) spotted on top of agar plates containing
474 E7 cells (BZB1011 pColE7) (a), E8 cells (BZB1011 pColE8) (b), or susceptible
475 cells (BZB1011) (c) and (d), after 12 hours at 37°C where the agar contained between 0 mm
476 and 333 mm arabinose. The agar plates were composed of 1.5% (w/v) of agar in LB (a)–(c) or
477 M9 (d).



480
 481 **Figure S5.** Co-culture of E7-inducible and susceptible cells. (a) Graph of the mean GFP and
 482 RFP expression of E7-inducible (green line) and S cells (red line), respectively, mixed
 483 homogeneously at equal starting ratios in M9 ultra low gelling temperature agarose (ULGA)
 484 gels at a combined cell starting density of 3.6×10^9 cells mL⁻¹ at varying arabinose
 485 concentrations after 18 hours at 37°C. (b) Graph of the number of micro-colonies formed of
 486 E7-inducible in M9 ULGA gels after 18 h at 37°C at varying arabinose concentrations at a
 487 cell starting ratio of 1.6×10^7 cells mL⁻¹. (c)-(e) Graphs of the number of micro-colonies
 488 formed of E7-inducible (green line) and S cells (red line) mixed homogeneously at starting
 489 ratios of 1:1 (equal number between E7-inducible and S cells), 1:9 or 1:99 (E7-inducible to S
 490 cells), respectively, in M9 ultra low gelling temperature agarose (ULGA) gels at a combined
 491 cell starting density of 1.6×10^7 cells mL⁻¹ at varying arabinose concentrations after 18 hours
 492 at 37°C. The solid line and shaded area represent the mean and standard deviation of $n = 4$
 493 technical replicates.



496

497

498

499

500

501

502

503

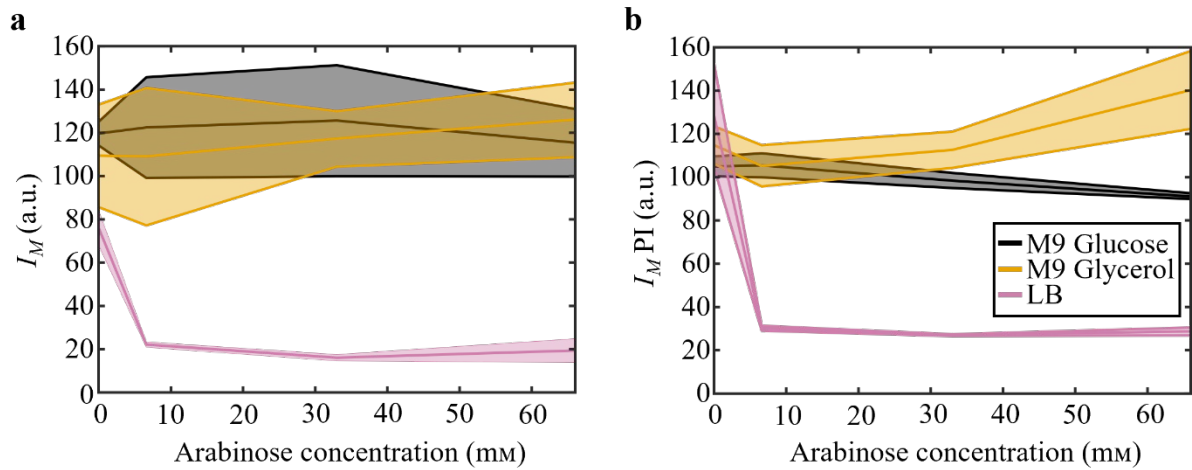
504

Figure S6. Time-dependent release of arabinose from droplet networks. (a) and (b) Box plots of the number of E7-inducible (BZB1011 pBAD-E7) (a) and susceptible cells (BZB1011) (b) arising from competition between them, when droplet networks containing either 0 mM or 33 mM arabinose and $50 \mu\text{g mL}^{-1}$ αHL were placed on top of the bacterium-laden hydrogel for 18 hours after placement immediately after gel formation (placed after 0 h) or placement after 24 hours of cell growth (placed after 24 h). The starting ratio was 1:9 (E7-inducible to susceptible cells) while the total starting cell density was 1.6×10^7 cells mL^{-1} . Individual data points on the box plots are technical replicates. (c) and (d) Box plots of the number of E7-

505 inducible (BZB1011 pBAD-E7) (c) and susceptible cells (BZB1011) (d) arising from
506 competition between them, when droplet networks containing 333 mM arabinose and
507 $50 \mu\text{g mL}^{-1}$ αHL were placed on top of the bacterium-laden hydrogel for 18 or 42 hours,
508 respectively. The starting ratio was 1:9 (E7-inducible to susceptible cells) while the total
509 starting cell density was 1.6×10^7 cells mL^{-1} . Individual data points on the box plots are
510 technical replicates.

511

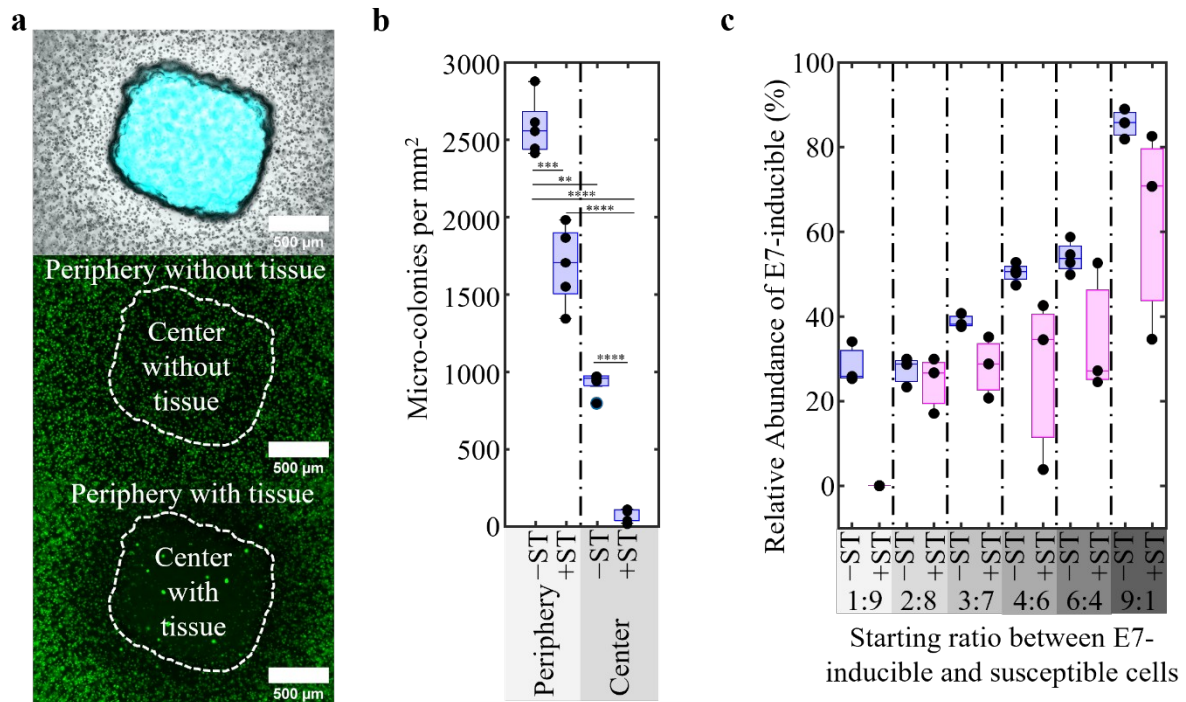
512



513

514 **Figure S7.** Importance of culture medium for colicin competition. (a) and (b) Graphs of the
515 mean sfGFP expression (a) and mean intensity of intracellular propidium iodide (b), in
516 ULGA gels composed of M9 supplemented with 24 mM glucose, M9 supplemented with
517 24 mM glycerol or LB at a range of arabinose concentrations (0 mM, 6 mM, 33 mM and
518 66 mM) after 18 hours at 37°C. The gels contained E7-inducible cells at a starting cell density
519 of 3.6×10^9 . The solid line and shaded area represent the mean and standard deviation of $n = 4$
520 technical replicates.

521



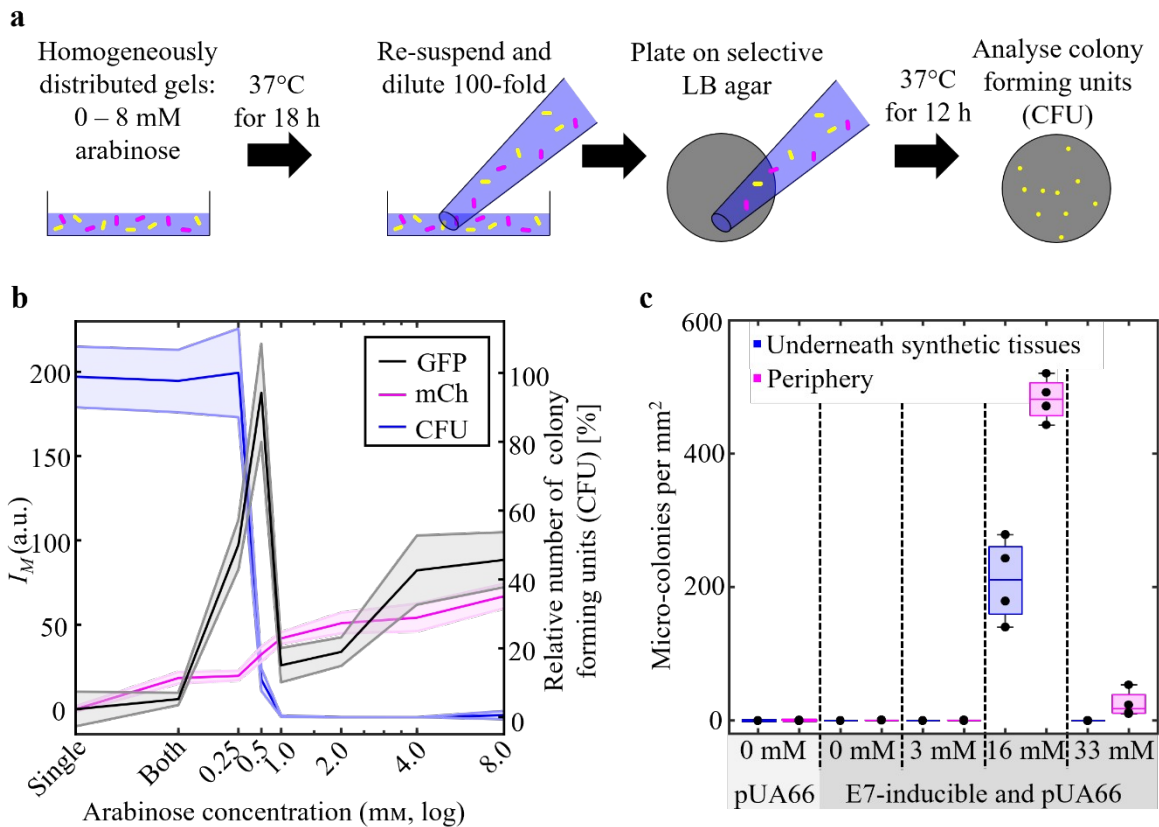
523

524

Figure S8. Localized expression of colicin E7 underneath droplet networks. (a) Composite microscope image (bright-field and cascade dextran blue, top image) of a droplet network on top of a bacterium-laden hydrogel and sfGFP fluorescence images of bacterium-laden hydrogel when a droplet network was placed (bottom image) and was not placed on top of the image (center image). The white dashed line represents the outline of the tissue, which was used as a reference area for when no droplet network was placed on top of the bacterium-laden hydrogel. The bacterium-laden hydrogels contained E7-inducible cells (BZB1011 pBAD-E7) at a starting cell density of 1.6×10^7 cells mL⁻¹. (b) Boxplot of the micro-colonies per mm² within the peripheral and central areas of E7-inducible cells (BZB1011 pBAD-E7) (**Figure S1(c)** and **Table S1**) seeded at a starting cell density of 1.6×10^7 cells mL⁻¹ in ULGA gels composed of LB medium at 37°C for 18 hours after droplet networks containing 333 mM arabinose and 50 μg mL⁻¹ αHL monomer were (+ST) and were not (-ST) placed on top of the bacterium-laden hydrogels. The individual data points are depicted for each condition with n = 5 technical replicates. It was tested whether the data was normally distributed using the Shapiro-Wilk test ($p < 0.05$). Given groups were normally distributed, significance between groups was tested performing a two-sample t-test. If data of at least one group was not normally distributed, significance between groups was tested by performing a Wilcoxon rank-sum test. ** $p < 0.01$, *** $p < 0.001$ and **** $p < 0.0001$. (c) Boxplot of the relative abundance (RA) of E7-inducible micro-colonies at a range of starting ratios (1:9 to 9:1, ratio between E7-inducible cells and susceptible cells) when droplet networks containing

544 333 mM arabinose and $50 \mu\text{g mL}^{-1}$ of αHL monomer were placed (+ST) or not placed (-ST)
545 on top of the bacterium-laden hydrogel after 18 hours at 37°C . The total starting cell density
546 was 1.6×10^7 cells mL^{-1} . Shown are individual data points of $n = 4$ technical replicates and
547 boxplots are mean and interquartile range.

548



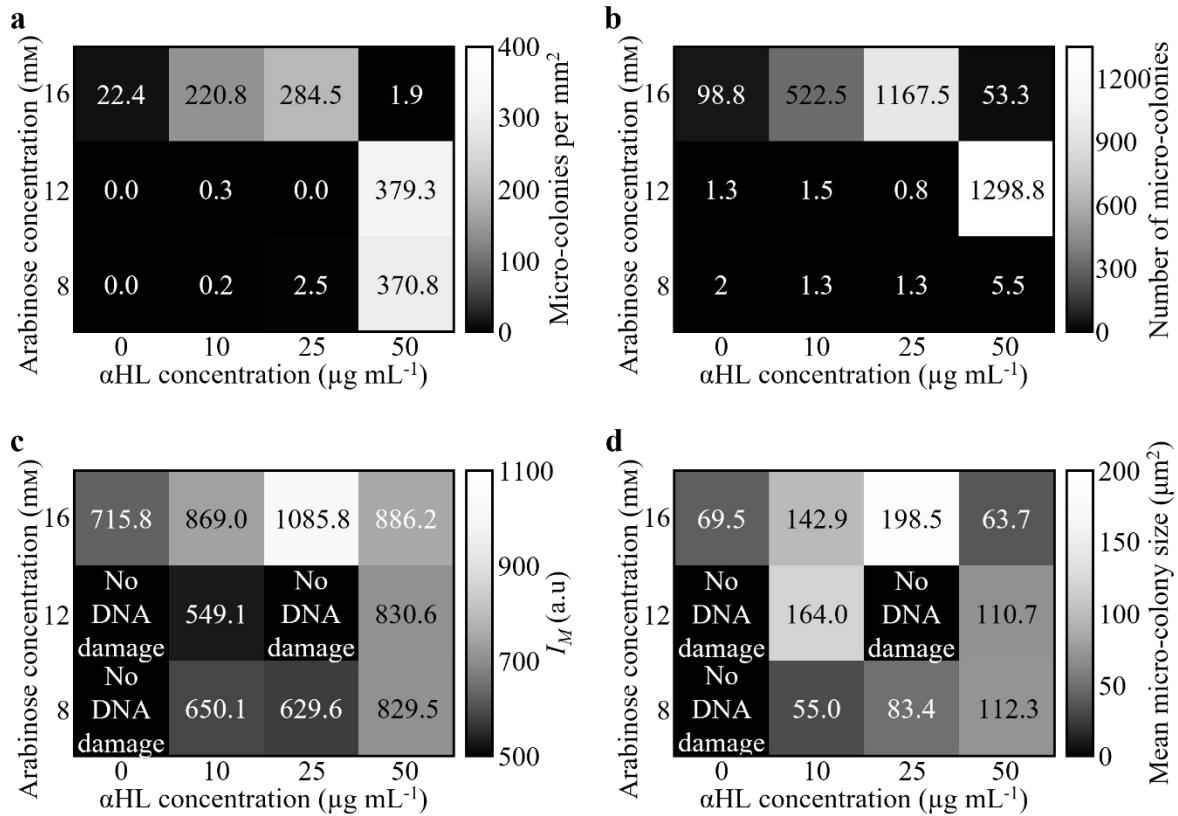
550

551 **Figure S9.** E7-inducible causes DNA damage in susceptible cells. (a) Schematic depicting
 552 the workflow to characterize the correlation between GFP expression and the relative colony
 553 forming units (CFU), whereby E7R-inducible or E7R-inducible and S-GFP cells are grown
 554 for 18 h at 37 °C in M9 ULGA gels, before re-suspension and plating on LB agar plates
 555 containing 50 $\mu\text{g mL}^{-1}$ of kanamycin to select for colony-forming units arising from S-GFP
 556 cells. (b) Graph of the mean mCherry expression (mean fluorescence intensity of activated
 557 pixels, indicating colicin E7 expression), mean sfGFP expression (indicating DNA damage in
 558 susceptible cells), and the relative number of colony forming units (CFU) from susceptible
 559 cells over a range of arabinose concentrations (0 mM to 8 mM) added to bacterium-laden
 560 hydrogels composed of M9 ULGA supplemented with 24 mM glycerol. The starting ratio
 561 between E7R-inducible and susceptible cells (BZB1011, S-GFP cells) was 1:1 at a total
 562 starting cell density of 1.6×10^7 cells mL^{-1} . Mean mCherry expression and mean GFP
 563 expression of E7-inducible and susceptible cells, respectively, were measured after 18 hours
 564 of co-culture, while the number of colony forming units from susceptible cells was measured
 565 12 hours after solubilization of the M9 ULGA gels and plating on selective medium. ‘Single’
 566 indicates M9 ULGA gels containing only susceptible cells seeded at 0.8×10^7 cells mL^{-1}
 567 without the addition of arabinose (0 mM), while ‘both’ indicates the co-culture of E7-

568 inducible and susceptible cells at an equal starting ratio and a total starting cell density of
569 1.6×10^7 cells mL⁻¹ without the addition of arabinose (0 mM). The solid line and shaded area
570 represent the mean and standard deviation of n = 4 technical replicates. (c) Boxplots of the
571 number of micro-colonies per mm² of activated susceptible cells (expressing GFP as a
572 consequence of DNA-damage) in areas underneath the droplet networks containing a range of
573 arabinose concentrations (0 mM – 33 mM) and 50 µg mL⁻¹ of αHL monomer, and peripheral
574 areas (outside of where the droplet networks were placed) at 18 hours after placement of
575 droplet networks at 37°C. E7R-inducible (BZB1011, E7R-inducible) and susceptible cells
576 (BZB1011, S-GFP cells) were seeded at a 1:1 starting ratio and a total starting cell density of
577 1.6×10^7 cells mL⁻¹. The ULGA gels contained M9 medium supplemented with 24 mM
578 glycerol. Shown are individual data points of n = 4 technical replicates and boxplots display
579 the mean and interquartile range.

580

581
582



583
584 **Figure S10.** Localized DNA damage in susceptible cells. (a)-(d) Heat-maps of micro-
585 colonies per mm² in areas underneath droplet networks (a), the total number of micro-
586 colonies in peripheral areas outside of where droplet networks were placed (b), the mean GFP
587 expression (c) and mean micro-colony size (d) of activated susceptible cells (S-GFP cells
588 experiencing DNA-damage caused by colicin E7 expressed from E7R-inducible) after 18
589 hours at 37°C. E7R-inducible cells (BZB1011, E7R-inducible) and susceptible cells
590 (BZB1011, S-GFP) were seeded at equal starting ratio and a total cell density of
591 1.6×10^7 cells mL⁻¹. The ULGA gels were composed of M9 supplemented with 24 mM
592 glycerol. Droplet networks contained a range of arabinose concentrations (8 mM, 12 mM and
593 16 mM) and a range of α HL monomer concentrations ($0 \mu\text{g mL}^{-1}$, $10 \mu\text{g mL}^{-1}$, $25 \mu\text{g mL}^{-1}$ and
594 $50 \mu\text{g mL}^{-1}$).

595

596 **Supplementary Tables**

597

598 **Table S1.** Summary of strains and plasmids.

	Strain and genotype	Recombinant DNA	Abbreviation	Promoter	Description	Source of recombinant DNA
1	BZB1011 <i>Pmax:sfgfp::Tn7</i>	pJS1- <i>PBAD</i> :- <i>mCherry</i> - AMP	mCherry- inducible	pBAD	Constitutive expression of sfGFP, induced expression of mCherry	This study
2	BZB1011 <i>Pmax:mrfp1::Tn7</i>	-	S	-	Constitutive expression of RFP	-
3	BZB1011 <i>Pmax:sfgfp::Tn7</i>	pKC1- <i>PBAD</i> :- <i>ColE7</i> -AMP	E7-inducible	pBAD	Constitutive expression of sfGFP, induced expression of colicin E7	This study
4	BZB1011 <i>Pmax:sfgfp::Tn7</i>	pYY1- <i>PBAD</i> :- <i>ColE7</i> - <i>mCherry</i> - AMP	E7R- inducible	pBAD	Constitutive expression of sfGFP, induced expression of colicin E7 and mCherry	This study
5	BZB1011	pUA66- <i>PcolE2::sfgfp</i> <i>p</i>	S-GFP	pColE2	Unlabeled, GFP expression upon sensed DNA- damage	[3,4]
6	BZB1011 <i>Pmax:mrfp1::Tn7</i>	pColE7	pcolE7	SOS	Constitutive expression of RFP, natural colicin E7 plasmid	[10]

7	BZB1011 <i>Pmax:mrfp1::Tn</i> 7	pColE8	pcolE8	SOS	Constitutiv ^[10] e expression of RFP, natural colicin E8 plasmid
---	---------------------------------------	--------	--------	-----	---

599 **Supplementary Methods**

600 **Growth overlay assay**

601 Plates for growth inhibition assay consisted of two layers of solidified agar. The bottom layer
602 did not contain cells, while the top layer contained bacterial cells. LB/M9 agar plates (1.5%
603 w/v) were prepared by pouring 20 mL of liquid LB/M9 per petri dish before drying in a
604 laminar flow hood. Overnight cultures of both the susceptible strain and toxin-expressing
605 strain were prepared by inoculation from glycerol stocks one day prior to the experiment.
606 Strains were grown in a tube containing 4 mL of LB on a shaker (225 rpm) at 37°C for no
607 longer than 12h, before the overnight culture of susceptible cells was inoculated at an OD of
608 0.05 in a tube containing 4 mL of LB and grown at 37°C with shaking (225 rpm). When
609 susceptible cells reached an OD of 0.6, 200 µL of the cell suspension was added to 6 mL of
610 melted LB/M9 agar (0.75% w/v) before pouring 6 mL of the resulting cell suspension per
611 petri dish on the dried 20 mL of LB/M9 agar. Both the bottom agar and top agar (containing
612 susceptible cells) of the LB/M9 agar plates contained arabinose concentrations of 0% w/v,
613 0.5% w/v, 1% w/v or 5% w/v. The plates were dried for 1 h. Once dried, 0.5 µL of the toxin-
614 expressing stain was pipetted on top of the LB/M9 agar plate in serial dilutions of
615 10⁰ (undiluted), 10⁻¹, 10⁻², 10⁻³ and 10⁻⁴. The plates were dried for 15 min before placed in a
616 static incubator at 37°C for 12 h. Plates were imaged using a gel imager and epi-fluorescent
617 microscope.

618

619 **Propidium iodide staining**

620 Cell death staining was performed using propidium iodide by preparing a stock
621 solution (1.5 mM) of propidium iodide in DMSO. Then, a working solution was prepared by
622 diluting the stock solution with H₂O to 150 µM. The working solution was added to the
623 bacterial cell suspension in M9 ULGA prior to gel solidification to reach a final concentration
624 of 5 µM.

625

626 **Determination of Relative Colony Forming Units (CFU)**

627 M9 ULGA gels (supplemented with 24 mM of glycerol) were formed containing E7-
628 inducible (“Single”) or E7-inducible and S-GFP cells at a starting ratio of 1:1 and a total
629 starting cell density of 1.6×10^7 cells mL⁻¹. The bacterial cells were cultured for 18 h at 37 °C
630 in the M9 ULGA gels supplemented by varying concentrations of arabinose (0 mM – 8 mM),
631 before re-suspending the bacterium-laden hydrogels by pipetting to form 100-fold dilutions.
632 Then, the bacterium-containing solutions were plated onto LB agar plates containing
633 50 µg mL⁻¹ of kanamycin, which selected for S-GFP cells. The LB agar plates were then
634 incubated for another 12 h at 37 °C, before the relative number of colony forming units
635 arising from S-GFP cells were determined according to equation S1.

636 **References**

- 637 [1] D. A. Siegele, J. C. Hu, *Proc Natl Acad Sci U S A* **1997**, *94*, 8168.
- 638 [2] A. Alcinesio, O. J. Meacock, R. G. Allan, C. Monico, V. Restrepo Schild, I. Cazimoglu,
639 M. T. Cornall, R. Krishna Kumar, H. Bayley, *Nat Commun* **2020**, *11*, 2105.
- 640 [3] E. T. Granato, K. R. Foster, *Current Biology* **2020**, *30*, 2836.
- 641 [4] D. A. I. Mavridou, D. Gonzalez, W. Kim, S. A. West, K. R. Foster, *Current Biology*
642 **2018**, *28*, 345.
- 643 [5] E. Cascales, S. K. Buchanan, D. Duché, C. Kleanthous, R. Lloubès, K. Postle, M. Riley,
644 S. Slatin, D. Cavard, *Microbiology and Molecular Biology Reviews* **2007**, *71*, 158.
- 645 [6] K. E. S. Avelar, L. J. F. Pinto, L. C. M. Antunes, L. A. Lobo, M. C. F. Bastos, R. M. C.
646 P. Domingues, M. C. De Souza Ferreira, *Letters in Applied Microbiology* **1999**, *29*, 264.
- 647 [7] L. M. Guzman, D. Belin, M. J. Carson, J. Beckwith, *J Bacteriol* **1995**, *177*, 4121.
- 648 [8] C. G. Miyada, L. Stoltzfus, G. Wilcox, *Proceedings of the National Academy of*
649 *Sciences* **1984**, *81*, 4120.
- 650 [9] “Benchling [Biology Software],” can be found under <https://benchling.com>, **2024**.
- 651 [10] L. Ghazaryan, L. Tonoyan, A. A. Ashhab, M. I. M. Soares, O. Gillor, *Arch Microbiol*
652 **2014**, *196*, 753.
- 653